

## Singularity spectra of rough growing surfaces from wavelet analysis

M. Ahr\* and M. Biehl

*Institut für Theoretische Physik, Julius-Maximilians-Universität Würzburg, Am Hubland, 97074 Würzburg, Germany*

(Received 13 January 2000)

We apply the *wavelet transform modulus maxima* method [A. Arnéodo, N. Decoster, and S. G. Roux, Phys. Rev. Lett. **83**, 1255 (1999)] to the analysis of simulated surfaces grown by molecular-beam epitaxy. In contrast to the structure function approach commonly used in the literature, this method permits an investigation of the complete singularity spectrum. We focus on a kinetic Monte Carlo model with Arrhenius dynamics, which in particular takes into consideration the process of thermally activated desorption of particles. We find a wide spectrum of Hölder exponents, which reflects the multiaffine surface morphology. Although our choice of parameters yields small desorption rates (<3%), we observe a dramatic change in the singularity spectrum, which is shifted toward smaller Hölder exponents. Our results offer a mathematical foundation of anomalous scaling: We identify the global exponent  $\alpha_g$  with the Hölder exponent that maximizes the singularity spectrum.

PACS number(s): 64.60.Ht, 05.40.-a, 05.70.Ln, 81.10.Aj

### I. INTRODUCTION

Inspired by the great technological importance of epitaxial crystal growth, the past decade has seen much theoretical research in the subject of kinetic roughening of surfaces during growth. The investigation of this effect, which is undesirable in practical applications, promises deep insight into statistical physics far from thermal equilibrium (see, e.g., [1] for an overview). We focus on a full-diffusion Monte Carlo model of homoepitaxial growth of a hypothetical material with simple cubic lattice structure under solid on solid conditions, i.e., the effects of overhangs and displacements are neglected. Then, the crystal can be described by a two-dimensional array of integers that denote the height  $f(\vec{x})$  of the surface. On each site, new particles are deposited with a rate  $r_a$ . Particles on the surface hop to nearest neighbor sites with Arrhenius rates  $\nu_0 \exp[-(E_b + nE_n)/(k_b T)]$ , where  $E_b$  and  $E_n$  are the binding energies of a particle to the substrate and to its  $n$  nearest neighbors,  $\nu_0$  is the attempt frequency, and  $k_b T$  has its usual meaning. In contrast to earlier investigations of similar models [2], we permit the desorption of particles from the surface with rates  $\nu_0 \exp[-(E_d + nE_n)/(k_b T)]$ , where  $E_d > E_b$ .

The aim of this publication is twofold: We will first discuss the advantages of the wavelet analysis compared to the structure function (SF) approach, which has to date been the only approach used in the investigation of multiaffine surfaces. Then we will apply this formalism to investigate the influence of desorption on kinetic roughening. We conclude with some remarks on the relevance of universality classes for our results.

### II. SCALING CONCEPTS

The standard approach of dynamic scaling [1] assumes that the statistical properties of a growing surface before saturation remain invariant under a simultaneous transforma-

tion of spatial extension  $\vec{x}$ , height  $f(\vec{x})$ , and time  $t$ ,

$$\vec{x} \rightarrow b\vec{x} = \vec{x}'; \quad f \rightarrow b^\alpha f = f'; \quad t \rightarrow b^z t = t'; \quad (1)$$

where  $b$  is an arbitrary positive constant. This implies that a part of the surface smaller than the correlation length  $\xi(t) \sim t^{1/z}$  can be regarded as self-affine with Hurst exponent  $\alpha$ . A popular method of measuring  $\alpha$  uses height-height correlation functions of (theoretically) arbitrary order  $q$ :

$$G(q, \vec{l}, t) := \langle |f(\vec{x}, t) - f(\vec{x} + \vec{l}, t)|^q \rangle_{\vec{x}} \sim l^{q\alpha} g(l/\xi(t)), \quad (2)$$

where  $g(x) \rightarrow \text{const}$  for  $x \rightarrow 0$  and  $g(x) \rightarrow \text{const} \times x^{-q\alpha}$  for  $x \rightarrow \infty$ . In practice,  $q=2$  is the most common choice.

In principle, there are two different ways to measure  $\alpha$ . The local approach determines  $\alpha$  from the initial slope of  $\ln[G(q, \vec{l}, t)]$  versus  $\ln(l)$  for small  $l$ . The global approach analyzes the dependence of the surface width  $w = \sqrt{\langle [f(\vec{x}, t) - \langle f(\vec{x}, t) \rangle]^2 \rangle_{\vec{x}}}$  in the saturation regime on the system size  $N$ :  $w_{sat}(N) \sim N^{\alpha_g}$ . Before saturation, the surface width increases like  $w \sim t^\beta$ , where  $\beta = \alpha/z$ . An alternative that avoids the simulation of different system sizes uses the complete functional dependence of Eq. (2):  $\alpha_g$  and  $z$  are chosen such that the curves of  $G(2, \vec{l}, t)/l^{2\alpha_g}$  versus  $l/t^{1/z}$  collapse on a unique function  $g$  within a large range of  $t$  and  $l$ .

However, a careful analysis of simulation data [3–5,2] has shown that several models of epitaxial growth show significant deviations from this simple picture. First, one obtains different values of  $\alpha$  from the local than from the global approach, a phenomenon that is called anomalous scaling. Second, one often finds multiscaling: height-height correlation functions of different order yield a hierarchy of  $q$ -dependent exponents  $\alpha(q)$ , when determined from the initial power-law behavior of  $G(q, \vec{l}, t)$ .

These observations can be interpreted within the mathematical framework of multifractality. The Hölder exponent  $[6,1,7,8] h(\vec{x}_0)$  of a function  $f$  at  $\vec{x}_0$  is defined as the largest exponent such that there exists a polynomial of order  $n$

\*Email address: ahr@physik.uni-wuerzburg.de

$\langle h(\vec{x}_0) \rangle$  and a constant  $C$  which yield  $|f(\vec{x}) - P_n(\vec{x} - \vec{x}_0)| \leq C|\vec{x} - \vec{x}_0|^{h(\vec{x}_0)}$  in the neighborhood of  $\vec{x}_0$ . The Hölder exponent is a local counterpart of the Hurst exponent: a self-affine function with Hurst exponent  $\alpha$  has  $h(\vec{x}) = \alpha$  everywhere. However, in the case of a multiaffine function different points  $\vec{x}$  might be characterized by different Hölder exponents. This general case is characterized by the singularity spectrum  $D(h)$ , which denotes the Hausdorff dimension of the set of points where  $h$  is the Hölder exponent of  $f$ .

### III. WAVELET APPROACH TO MULTIFRACTALITY

There is a deep analogy between multifractality and thermodynamics [1,9,10], where the scaling exponents play the role of energy, the singularity spectrum corresponds to entropy, and  $q$  plays the role of inverse temperature. So theoretically  $D(h)$  might be calculated via a Legendre transform of  $\alpha(q): D(h) = \min_q(qh - q\alpha(q) + 2)$  [6–8], a method that has been called the structure function approach. However, its practical application raises fundamental difficulties. First, to obtain the complete singularity spectrum, one needs  $\alpha(q)$  for positive and negative  $q$ . But as  $|f(\vec{x}, t) - f(\vec{x} + \vec{l}, t)|$  might become zero,  $G(q, \vec{x}, t)$  is in principle undefined for  $q < 0$ . Therefore, only the left, ascending part of  $D(h)$  is accessible to this method. Additionally, the results of the SF method can easily be corrupted by polynomial trends in  $f(\vec{x})$  [7]. It might be due to these difficulties, that—to our knowledge—no attempt to determine the singularity spectrum of growing surfaces from  $\alpha(q)$  has ever been made. Although it has been argued that the  $\alpha(q)$  collapse onto a single  $\alpha$  in the limit  $t \rightarrow \infty$ , which characterizes the asymptotic universality class of the model [2,5,11], we are convinced that deeper insight into fractal growth on experimentally relevant finite time scales can be gained from a detailed knowledge of the  $D(h)$  spectrum.

To this end, we follow the strategy suggested by Arnéodo *et al.* [6,12,7], which circumvents the problems of the SF approach and permits a reliable measurement of the complete  $D(h)$ . Mathematically, the wavelet transform of a function  $f(\vec{x})$  of two variables is defined as its convolution with the complex conjugate of the wavelet  $\psi$ , which is dilated with the scale  $a$  and rotated by an angle  $\theta$  [12]:

$$T_{\psi}[f](\vec{b}, \theta, a) = C_{\psi}^{-1/2} a^{-2} \int d^2x \psi^*(a^{-1} \mathbf{R}_{-\theta}(\vec{x} - \vec{b})) f(\vec{x}). \quad (3)$$

Here  $\mathbf{R}_{\theta}$  is the usual two-dimensional rotation matrix, and  $C_{\psi} = (2\pi)^2 \int d^2k |\vec{k}|^{-2} |\hat{\psi}(\vec{k})|^2$  is a normalization constant, whose existence requires square integrability of the wavelet  $\psi(\vec{x})$  in Fourier space. Apart from this constraint, the wavelet can (in principle) be an arbitrary complex valued function. Introducing the wavelet  $\psi_{\delta}(\vec{x}) = \delta(\vec{x}) - \delta(\vec{x} + \vec{n})$ , where  $\vec{n}$  is an arbitrary unit vector, one easily obtains

$$\begin{aligned} T_{\psi_{\delta}}[f](\vec{b}, \theta, a) &= C_{\psi_{\delta}}^{-1/2} [f(\vec{b}) - f(\vec{b} + a \mathbf{R}_{\theta} \vec{n})] \\ &\Rightarrow \int d^2b |T_{\psi_{\delta}}[f](\vec{b}, \theta, a)|^q G(q, a \mathbf{R}_{\theta} \vec{n}). \end{aligned} \quad (4)$$

Consequently, a calculation of the moments of the wavelet transform of the surface yields the SF approach as a special case. To avoid its weaknesses, two major improvements are necessary.

First, we use a class of wavelets with a greater number of vanishing moments  $n_{\vec{\psi}}$  than  $\psi_{\delta}(\vec{x})$ . This increases the range of accessible Hölder exponents and improves the insensitivity to polynomial trends in  $f(\vec{x})$ . We introduce a two-component version of the wavelet transform,

$$\vec{T}_{\vec{\psi}}[f](\vec{b}, a) = \frac{1}{a^2} \int d^2x \begin{pmatrix} \Psi_1(a^{-1}(\vec{x} - \vec{b})) \\ \Psi_2(a^{-1}(\vec{x} - \vec{b})) \end{pmatrix} f(\vec{x}), \quad (5)$$

where the analyzing wavelets  $\Psi_1$  and  $\Psi_2$  are defined as partial derivatives of a radially symmetrical convolution function  $\Phi(\vec{x})$ :  $\Psi_1(\vec{x}) = \partial\Phi/\partial x$ ,  $\Psi_2(\vec{x}) = \partial\Phi/\partial y$ . Then  $\vec{T}_{\vec{\psi}}[f](\vec{b}, a)$  can be written as the gradient of  $f(\vec{x})$ , smoothed with a filter  $\Phi$  with respect to  $\vec{b}$ . This definition becomes a special case of Eq. (3) when multiplied by  $\vec{n}_{\theta} = (\cos(\theta), \sin(\theta))^T$ , yet allows for an easier numerical computation.<sup>1</sup> For example,  $\Phi$  can be a Gaussian, where  $n_{\vec{\psi}} = 1$ , or  $\Phi_1(\vec{x}) = (2 - \vec{x}^2) \exp(-\vec{x}^2/2)$ , which has two vanishing moments.

Second, the integration over  $\vec{b}$  in Eq. (4) is undefined for  $q < 0$ , since the wavelet coefficients might become zero. The basic idea is to replace it with a discrete summation over an appropriate partition of the wavelet transform that obtains nonzero values only, but preserves the relevant information on the Hölder regularity of  $f(\vec{x})$ . In the following, we will give a brief outline of the rather involved algorithm and refer the reader to [6,12,7] for more details and a mathematical proof. The wavelet transform modulus maxima (WTMM) are defined as local maxima of the modulus  $M_{\vec{\psi}}[f](\vec{b}, a) := |\vec{T}_{\vec{\psi}}[f](\vec{b}, a)|$  in the direction of  $\vec{T}_{\vec{\psi}}[f](\vec{b}, a)$  for fixed  $a$ . These WTMM lie on connected curves, which trace structures of size  $\sim a$  on the surface. The strength of each is characterized by the maximal value of  $M_{\vec{\psi}}[f](\vec{b}, a)$  along the line, the so-called wavelet transform modulus maxima maximum (WTMMM) [6]. While proceeding from large to small  $a$ , successively smaller structures are resolved. Connecting the WTMMM at different scales yields the set  $\mathcal{L}$  of maxima lines  $l$ , which leads to the locations of the singularities of  $f(\vec{x})$  in the limit  $a \rightarrow 0$ . The partition functions

$$\begin{aligned} Z(q, a) &= \sum_{l \in \mathcal{L}(a)} (\sup_{(\vec{b}, a') \in l, a' \leq a} M_{\vec{\psi}}[f](\vec{b}, a'))^q \\ &\sim a^{\tau(q)} \quad \text{for } a \rightarrow 0 \end{aligned} \quad (6)$$

<sup>1</sup>For simplicity, the irrelevant constant  $C_{\psi}$  has been omitted.

are defined on the subset  $\mathcal{L}(a)$  of lines that cross the scale  $a$ . From the analogy between the multifractal formalism and thermodynamics,  $D(h)$  is calculated via a Legendre transform of the exponents  $\tau(q)$  that characterize the scaling behavior of  $Z(q, a)$  on small scales  $a$ :  $D(h) = \min_q (qh - \tau(q))$ . Additionally,  $\tau(q)$  itself has a physical meaning for some  $q$ :  $-\tau(0)$  is the fractal dimension of the set of points where  $h(\vec{x}) < \infty$ , while the fractal dimension of the surface  $f(\vec{x})$  itself equals  $\max(2, 1 - \tau(1))$ .

#### IV. RESULTS

In our simulations, we choose the parameters  $\nu_0 = 10^{12}/s$ ,  $E_b = 0.9$  eV, and  $E_n = 0.25$  eV, and a temperature  $T = 450$  K. To study the influence of desorption, we consider three models with different activation energies  $E_d$ . In model A desorption is forbidden, i.e.,  $E_d = \infty$ . Models B and C have  $E_d = 1.1$  eV and  $E_d = 1.0$  eV. We simulate the deposition of  $2 \times 10^4$  monolayers at a growth rate of one monolayer per second on a lattice of  $N \times N$  unit cells using periodic boundary conditions, our standard value being  $N = 512$ . To check for finite size effects, we have also simulated  $N = 256$ . In all results presented averages over six independent simulation runs have been performed. Although we have used an optimized algorithm, these simulations consumed several weeks of CPU time on our workstation cluster.

First, we checked our results for artifacts resulting from properties of the analyzing wavelet rather than from the analyzed surface by using different convolution functions  $\Phi_n$ :  $\Phi_0$  is the Gaussian function,  $\Phi_n, n \geq 1$  are products of Gaussians and polynomials, which have been chosen such that the first  $n$  moments vanish. Then the analyzing wavelets have  $n\tilde{\nu}_n = n + 1$  vanishing moments. We find [Fig. 1(a)] that the  $\tau(q)$  curve obtained with  $\Phi_0$  deviates significantly from those obtained with  $\Phi_1$ ,  $\Phi_2$ , and  $\Phi_3$ . The latter agree apart from small differences that are mainly due to the discrete sampling of the wavelet in the numerical implementation of the algorithm. This is explained by the theoretical result [8] that  $d\tau(q)/dq = n\tilde{\nu}$  for  $q < q_{crit} < 0$  if the number of vanishing moments of the analyzing wavelet is too small. Consequently, the agreement of the other curves proves their physical relevance.

Figure 1(b) shows averages of  $\tau(q)$  curves obtained with the convolution functions  $\Phi_1$ ,  $\Phi_2$ , and  $\Phi_3$  from surfaces after  $2 \times 10^4$  s of growth on an initially flat substrate. For all our models, their nonlinear behavior reflects the multiaffine surface morphology. From the fact that these curves are reproduced within statistical errors in simulations with  $N = 256$ , we conclude that finite size effects can be neglected. Clearly, desorption reduces the slope of  $\tau(q)$ , although only a small fraction of the incoming particles is desorbed: 0.18% in model B and 2.57% in model C with slightly higher values at earlier times. The corresponding singularity spectra are shown in Fig. 2(a). They have a typical shape whose descending part seems to be symmetrical with the ascending part and which changes at most slightly, while the whole spectra are shifted toward smaller Hölder exponents as desorption becomes more important. We emphasize that we find no evidence for a time dependence of the singularity spectra within the range  $9700 \leq t \leq 2 \times 10^4$  s, so that our re-

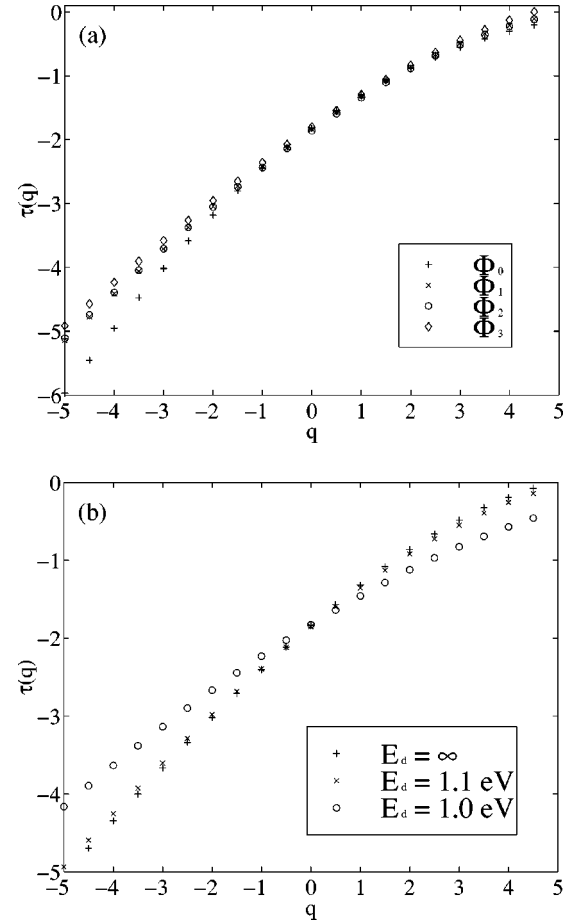


FIG. 1. (a)  $\tau(q)$  in the  $E_d = \infty$  model as obtained from investigations with different wavelets. Note the deviations of the data obtained with the Gaussian function  $\Phi_0$ . (b)  $\tau(q)$  for models with different activation energies  $E_d$  of desorption. All data have been obtained from surfaces after  $2 \times 10^4$  s of simulated time. Sizes of error bars are on the order of symbol sizes.

sults do not support the idea of an asymptotic regime characterized by a single exponent  $\alpha$ . However, the accessible time range of computer simulations is limited, so that we cannot finally disprove the existence of such a regime.

The multifractal formalism has replaced the unique scaling exponent  $\alpha$  of spatial extension in the simple picture of dynamic scaling [Eq. (1)] with a wide spectrum of Hölder exponents. By analogy, one might find it necessary to replace the scaling exponent  $\beta$  with a distribution of temporal counterparts of  $h$ . To answer this question, we investigate the probability distribution function (PDF)  $P(f - \langle f \rangle, t)$  of surface heights. Dynamical scale invariance with a single  $\beta$  demands that

$$P(f - \langle f \rangle, t) = \tilde{P} \left( \frac{f - \langle f \rangle}{t^\beta} \right) \frac{1}{t^\beta}, \quad (7)$$

i.e., the rescaled PDFs  $Pt^\beta$  should collapse onto a single function  $\tilde{P}$  when plotted as a function of  $(f - \langle f \rangle)/t^\beta$  within a large time range.

We measure  $\beta$  from the increase of the surface width with time, which follows a power law for  $t \geq 150$  s in models A and B ( $\beta_A = 0.19 \pm 0.01$ ,  $\beta_B = 0.17 \pm 0.01$ ) respectively

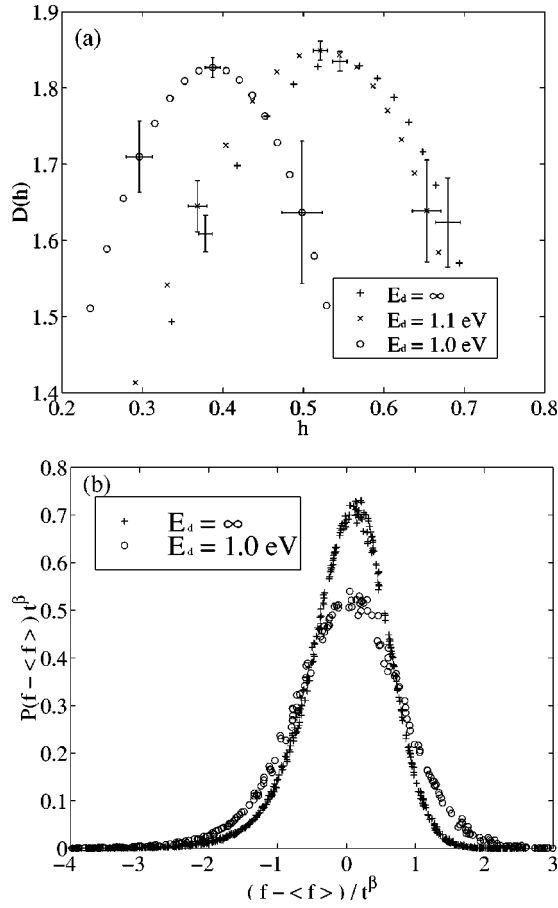


FIG. 2. (a) Singularity spectra obtained from a Legendre transform of the data in Fig. 1(b). (b) Data collapse of rescaled PDFs of surface heights for times between 150 and  $2 \times 10^4$  s (model A) and 150 and 7500 s (model C). We have used  $\beta = 0.188$  for model A with  $E_d = \infty$  and  $\beta = 0.109$  for model C ( $E_d = 1.0$  eV). Time is measured in seconds.

150 <  $t$  < 7500 s in model C ( $\beta_C = 0.11 \pm 0.01$ ), which then starts to approach the final saturation regime. The high quality of the data collapse of the PDFs shown in Fig. 2(b) proves that the scaling form (7) holds, showing that a single exponent describes the scaling behavior of  $P(f - \langle f \rangle, t)$ . This parallels the finding of Krug in [4] for the one-dimensional Das Sarma–Tamborenea model.

Finally, the WTMM method, which is a precise tool to investigate local scaling properties of surfaces, might help to get some insight into the phenomenon of anomalous scaling. The conventional picture [13–15] notes the difference between the global  $\alpha_g$  and a ‘‘local  $\alpha$ ’’ that is determined from the power-law behavior of  $G(2, \vec{l}, t)$  for small  $l$ , and, within the multifractal formalism, simply corresponds to a Hölder exponent on the ascending part of the singularity spectrum. We have determined the global scaling exponents  $\alpha_g$  and  $z$  from the data collapse of the scaled height-height correlation function  $G(2, \vec{l}, t)$  and find agreement within statistical errors between  $\alpha_g$  and that value of the Hölder exponent  $h_m$  which maximizes  $D(h)$  (Table I). This empirical result can be explained with a saddle-point argument. We calculate the surface width

TABLE I. Simulation results:  $p_d$  is the fraction of particles that desorbs,  $\beta$  is the scaling exponent of the PDF of surface heights,  $h_m$  is the Hölder exponent that maximizes  $D(h)$ ,  $\alpha_g$  and  $z_g$  are the global scaling exponents of  $G(2, \vec{l}, t)$ , and  $D_f$  is the fractal dimension of the surface.

Model	$p_d$	$\beta$	$h_m$	$\alpha_g$	$z_g$	$D_f$
A	0	$0.19 \pm 0.01$	$0.54 \pm 0.01$	0.55	2.9	$2.32 \pm 0.01$
B	0.18%	$0.17 \pm 0.01$	$0.52 \pm 0.01$	0.51	3.3	$2.35 \pm 0.01$
C	2.57%	$0.11 \pm 0.01$	$0.38 \pm 0.01$	0.39	3.5	$2.45 \pm 0.02$

$$w^2 = \frac{1}{N^2} \int d^2x [f(\vec{x}) - \langle f \rangle]^2$$

$$= \frac{1}{N^2} \int d\tilde{h} \int d^2x \delta(\tilde{h} - h(\vec{x})) [f(\vec{x}) - \langle f \rangle]^2. \quad (8)$$

Since the last integral  $[I(\tilde{h})]$  grows like  $N^{D(\tilde{h})}$  with the system size, in large systems the integral over  $\tilde{h}$  will be dominated by  $I(h_m)$ . That means that  $w$  and therefore the global scaling properties of the surface are governed by the subset of points that has the greatest fractal dimension. Consequently, the surface will behave like a self-affine surface with Hurst exponent  $h_m$  on length scales comparable to the system size.

## V. CONCLUSIONS

Table I summarizes our results. Model A without desorption recalls the results in [2], which were obtained with slightly different activation energies on smaller systems and shorter time scales. Models B and C show that desorption is an important process, which, although it affects only a small fraction of the adsorbed particles, must not be neglected, since it alters the scaling properties of the surfaces by reducing  $\beta$  and by shifting the singularity spectrum toward smaller Hölder exponents. Since the scaling behavior depends strongly on the height of the energy barrier of desorption, and the singularity spectra have no measurable tendency to narrow with time, our results cannot be used to make any decision about the asymptotic universality class of the investigated model. However, they show that the paradigm of a few universality classes characterized by a small number of exponents that are independent of details of the model is not adequate to describe the features of kinetic roughening on experimentally relevant time scales of a few hours of growth.

We are convinced that the application of mathematical tools like the wavelet analysis will help find a better description of fractal growth phenomena in the future.

## ACKNOWLEDGMENTS

We thank A. Arnéodo and J. M. López for providing us recent manuscripts before publication and A. Freking for a critical reading of the manuscript.

- [1] A.-L. Barabási and H. E. Stanley, *Fractal Concepts in Surface Growth* (Cambridge University Press, Cambridge, England, 1995).
- [2] S. Das Sarma, C. J. Lanczycki, R. Kotlyar, and S. V. Ghaisas, *Phys. Rev. E* **53**, 359 (1996).
- [3] A.-L. Barabási, R. Bourbonnais, M. Jensen, J. Kertész, T. Vicsek, and Y.-C. Zhang, *Phys. Rev. A* **45**, R6951 (1992).
- [4] J. Krug, *Phys. Rev. Lett.* **72**, 2907 (1994).
- [5] S. Das Sarma and P. Punyindu, *Phys. Rev. E* **55**, 5361 (1997).
- [6] A. Arnéodo, N. Decoster, and S. G. Roux, *Phys. Rev. Lett.* **83**, 1255 (1999); A. Arnéodo, N. Decoster, and S. G. Roux, *Eur. Phys. J. B* **15**(3), 567 (2000); S. G. Roux, A. Arnéodo, and N. Decoster, *Eur. Phys. J. B* **15**(4), 767 (2000); N. Decoster, S. G. Roux, and A. Arnéodo, *Eur. Phys. J. B* **15**(4), 739 (2000).
- [7] E. Bacry, J. F. Muzy, and A. Arnéodo, *J. Stat. Phys.* **70**, 635 (1992).
- [8] J. F. Muzy, E. Bacry, and A. Arnéodo, *Phys. Rev. E* **47**, 875 (1993).
- [9] M. Schroeder, *Fractals, Chaos, Power Laws: Minutes from an Infinite Paradise* (Freeman, New York, 1990).
- [10] T. Viscek, *Fractal Growth Phenomena* (World Scientific, Singapore, 1992).
- [11] C. Dasgupta, J. M. Kim, M. Dutta, and S. Das Sarma, *Phys. Rev. E* **55**, 2235 (1997).
- [12] J. C. Van Den Berg, *Wavelets in Physics* (Cambridge University Press, Cambridge, England, 1999).
- [13] J. M. López and M. A. Rodriguez, *Phys. Rev. E* **54**, R2189 (1996).
- [14] J. M. López, M. A. Rodriguez, and R. Cuerno, *Phys. Rev. E* **56**, 3993 (1997).
- [15] J. M. López, *Phys. Rev. Lett.* **83**, 4594 (1999); J. J. Ramasco, J. M. López, and M. A. Rodriguez, *Phys. Rev. Lett.* **84**, 2199 (2000).